The Need for a Universal Cloud Property Algorithm for Active Remote Sensors

K. Sassen and Z. Wang
University of Utah
Salt Lake City, Utah

Introduction

Lidar and radar measurements of cloud properties (e.g., cloud boundaries, phase, vertically resolved and integrated mass content, optical depth, etc.) are increasingly being relied on in modern climate-related research programs and are a keystone of the Atmospheric Radiation Measurement (ARM) Cloud and Radiation Testbed (CART) atmospheric measurement philosophy, to provide, relatively inexpensively, crucial cloud characterizations on a more or less routine continuous basis. As a result, a variety of data interpretation schemes and specific algorithms have been developed and are being applied to remote sensing data sets, but it must be recognized that a helter-skelter approach involves dangers as well as promise. It is clear that remote sensors can have vastly different operating characteristics and sensitivities to hydrometeors, so the derived data quantities in any particular case may be quite specific to the instrument and analysis method employed. This has the potential of misleading data users in the theoretical community. As our ice, water, and mixed-phase cloud algorithm developmental research continues, an important step we are currently taking is to provide to the community a "universal" cloud boundary (i.e., cloud base and top, along with cloud phase separation for precipitating clouds) algorithm. We briefly outline this algorithm here.

Review of Cloud Boundary Determination

As described by Platt et al. (1994), during the Experimental Cloud Lidar Pilot Study (ECLIPS) three basic methods were applied to the determination of cloud boundaries: the differential zero-crossing method (Pal and Cho 1992), the threshold method, and a quantitative approach based on the clear-air assumption (Sassen et al. 1992). The first two algorithms are related as they both discriminate a change of slope in the decreasing backscatter with altitude below cloud base, from the typically sharp increase in backscatter above cloud base. Both algorithms need careful tuning, however, to ignore small enhancements in backscatter caused by aerosols and noise. These methods also inherently depend on the shape of backscattered return and the vertical resolution of the system. The third method avoids some of these problems, but is strictly only useful for detecting relatively thin cirrus clouds.

Young (1995) used an alternative cloud-detection algorithm for thin clouds, where the cloud base and top are determined by extrapolating the reference cloud-free signal. Recently, Campbell et al. (1998) developed the Goddard Space Flight Center (GSFC) cloud boundary height algorithm for ARM VAP processing, which uses bi-directional vertical differencing of adjacent range bins from 1-minute shot averages compared to a similarly analyzed clear-sky baseline profile. An alternate approach to

determining cloud boundaries in radar and lidar data was offered recently by Clothiaux et al. (1995, 1998). Uttal et al. (1993) used a similar idea in their cloud boundary detection algorithm for vertically pointing radar data.

Unfortunately, there is no universal algorithm that is suitable for all situations, has the ability to deal with signal quality, and to differentiate between various targets such as clouds, virga, and aerosols. We are currently developing a more general algorithm for active remote sensors.

The Algorithm Flowchart

In this general algorithm, we start from the characters of backscattering like the slope (Pal et al. 1992) and "threshold" methods (Platt et al. 1994), but we take into account the underlying physics of the differences between cloud layers, aerosol layers, and noise effects. Figure 1 shows the flowchart of this general algorithm.

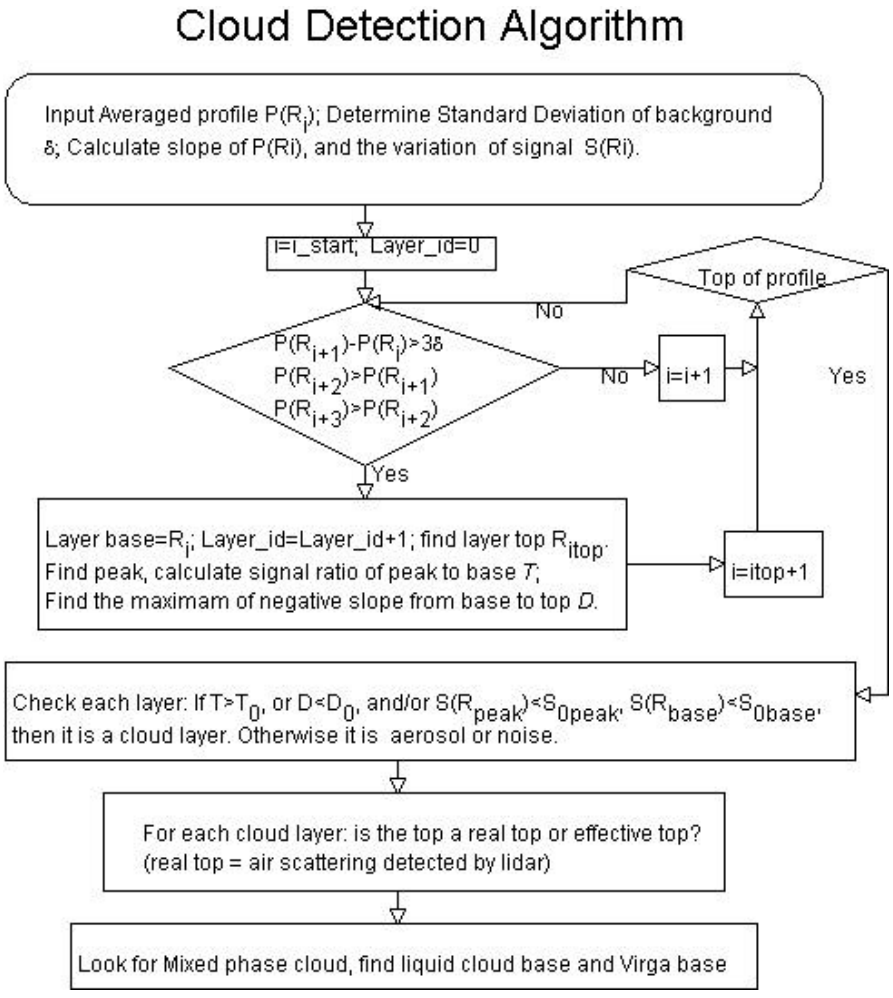

Figure 1. The flowchart of the basic algorithm.

Five Easy Steps of This Algorithm

The first step is to calculate the slope and the quality of the signal, and the standard deviation of the background noise level δ using a range-uncorrected averaged signal. To calculate the slope, we fit $\log(P(R_i))$ with R_i to a linear function, where P is power and R is altitude. The number of points used for fitting depends on the vertical resolution of systems. Points within 100 m to 200 m work for most systems. To characterize the quality of the signal, we calculate $S(R_i)$, the variation of the signal, defined by following equation:

$$S(R_i) = \frac{\sum_{j=i-n/2}^{i+n/2} \mathrm{abs}\left(\log\left(P(R_j)\right) - a - bR_j\right)}{\sum_{j=i-n/2}^{i+n/2} \log\left(P(R_j)\right)}$$

where a and b are coefficients from fitting $P(R_{i-n/2})$, ... $P(R_i)$, ... $P(R_{i+n/2})$ to a linear function: $\log(P(R_i)) = a + bR_i$. We will use this parameter to control the effects of noise. In this algorithm, we also define a minimum reliable signal P_{min} for the averaged signal of a given system. If the signal is below P_{min}, it is considered to be too noisy for analysis; P_{min} should be larger than 3δ.

The second step is to examine the signal upward and record possible layer and layer-related properties: height of layer-base, -peak, and -top, the ratio of peak signal to the signal of layer base, and the maximum negative slope within this layer. The identified layer could be a cloud layer, an aerosol layer, or a noise peak. Layer base is where the signal starts to increase in terms of the signal slope, and top is where the signal returns to the molecular level or noise level. The initial increase at layer base is larger than 3δ. The layer base should also satisfy the condition that the signal does not decrease to the base level in a short range after the initial increase for high vertical resolution measurement, because this signal may be a noise peak. So for high-resolution systems, we use at least three points of continuous increase to select a layer base, but for low vertical resolution systems, this is not required. To search for a layer top, we look for the altitude where the slope of signal returns to the slope of the clear-sky signal or the magnitude of signal reduces below P_{min}. This method can process any combination of cloud and aerosol layers.

The third step is to distinguish a cloud layer from an aerosol layer or noise. Aerosols are often stratified in the troposphere and cause similar features in backscattering like clouds. The main difference between cloud layer and aerosol layers are different magnitudes of the extinction and backscattering coefficients. If we neglect the effect of range and attenuation, then the ratio of peak signal to the layer base signal T is:

$$T = \frac{P_{peak}}{P_{base}} \approx \frac{\beta_{peak}}{\beta_{base}}$$

where β is backscattering coefficient. Most clouds are considerably thicker than aerosols at the same altitude, and since thin cirrus clouds only occur at high altitudes, it is straightforward to pre-select a

value for this ratio to distinguish these layers. For a 0.532-μm high vertical resolution lidar, for example, we select 4 for R<5 km and 1.5 for R>5 km as the thresholds for T to distinguish cloud from aerosol layers. The maximum of negative slope D is also a good parameter to distinguish a cloud from aerosol or noise. If D<-7 and R>0.5 km, a cloud layer is typically present in a lidar return. If T and D are below their thresholds, we regard the target as an aerosol layer or noise. These pre-selected values should change with wavelength and vertical resolution of the system because the optical properties of molecules, aerosols, and clouds have different wavelength dependence, and low vertical resolution systems detect smoother cloud signals than using high vertical resolution. S(R) is an excellent indicator of the effect of noise. If S(R) is larger than a given threshold, but T and D is too small, it is highly likely that the detected layer is generated by noise. This layer should be rejected.

The fourth step is to judge whether the cloud top is a real top or effective top height. In many cases involving optically thick clouds, lidar cannot penetrate the cloud layer, so the detected cloud top is an effective top. If the signal above cloud top is below P_{min} with a slope of about zero, the cloud top is possibly an effective top. On other hand, if the signal above cloud top is larger than P_{min} and with a negative slope around the slope of the air backscattering signal, the cloud top represents the actual top. Multiple scattering will present some problems for this analysis using some systems in very dense clouds.

The fifth step is to distinguish the cloud base from virga base for mixed-phase clouds or drizzle. Although the lidar signal from virga can also increase with height, its slope is much smaller than the slope of the signal at cloud base. On the other hand, dense clouds can attenuate lidar signal very rapidly. The change of positive slope in virga to cloud, and the strong negative slope in the clouds, give us important information to distinguish cloud-base from virga-base altitudes.

This general algorithm can also be used for radar signal analysis with some modifications. For radar measurements, we only need consider the first three steps. To derive more complete information about the cloud-top height, we need to combine the lidar and radar measurements. To classify clouds into different categories, we need more information, like the depolarization of the lidar return signal.

Future Steps

This algorithm is still under development. For more details, updated information, and results from this algorithm, check our web site located at http://www.met.utah.edu/ksassen/cloud/cld_detect.html. This algorithm is an important step toward development of a universal cloud property retrieval algorithm by combining active remote sensors and passive remote sensors. Our ultimate goal is to combine CART Raman Lidar, Millimeter-Wavelength Cloud Radar, dual-channel Microwave Radiometer, and mid-infrared effective column temperature to achieve a reliable characterization of cloud and aerosol properties.

References

Campbell, J. R., D. L. Hlavka, J. D. Spinhirne, D. D. Turner, and C. J. Flynn, 1998: Operational cloud boundary detection and analysis from micro pulse lidar data. In *Proceedings of the Eighth Atmospheric Radiation Measurement (ARM) Science Team Meeting*, DOE/ER-0738, pp. 119-122. U.S. Department of Energy, Washington, D.C.

Clothiaux, E. E., G. G. Mace, T. P. Ackerman, T. J. Kane, J. D. Spinhirne, and V. S. Scott, 1998: An automated algorithm for detection of hydrometer returns in micropulse lidar data. *J. Atmos. Oceanic Technol*., **15**, 1035-1042.

Clothiaux, E. E., M. A. Miller, B. A. Albrecht, T. P. Ackerman, J. Verlinde, D. M. Babb, R. M. Peters, and W. J. Syrett, 1995: An evaluation of 94-GHz radar for remote sensing of cloud properties. *J. Atmos. Oceanic Technol*., **12**, 201-229.

Pal, S. R., W. Steinbrecht, and A. I. Carswell, 1992: Automated method for lidar determination of cloud base height and vertical extent. *Appl. Opt*., **31**, 1488-1494.

Platt, C.M.R. et al., 1994: The experimental cloud lidar pilot study (ECLIPS) for cloud-radiation research. *Bull. Amer. Meteor. Soc*., **75**, 1635-1645.

Sassen, K., and B. S. Cho, 1992: Subvisual-thin cirrus lidar dataset for satellite verification and climatological research. *J. Appl. Meteor*., **31**, 1275-1285.

Uttal, T., L. I. Church, B. E. Martner, and J. S. Gibson, 1993: CLDSTATS: a cloud boundary detection algorithm for vertically pointing radar data. *NOAA Technical Memorandum ERL WPL-233*.

Young, S. A., 1995: Analysis of lidar backscatter profiles in optically thin clouds. *Appl. Opt*., **34**, 7019-7031.